Harmonic Analysis of Eddy Current Loss for Magnetic Thrust Bearings

Tian Yongsheng[1,a], Sun Yanhua[1,b], Yu Lie[1,c]

[1]Institute of Mechatronics and Information Systems, Key Laboratory of Ministry of Education for Strength and Vibration, Xi'an Jiaotong University, Xi'an, 710049, China

[a]yongsheng0220@163.com, [b]sunyanhua@mail.xjtu.edu.cn, [c]yulie@mail.xjtu.edu.cn

Abstract: In MTBs, high eddy current loss will be produced in the solid stator and thrust disk. They play a significant role in limiting the high-speed operation of rotating actuators. In this paper, the flux path of a MTB was divided into six elementary parts according to the distributions of flux. A frequency model of eddy current losses for every iron part was proposed and the boundary condition was defined by a fractional transfer function. Results from FEM show its validity.

Keywords: Magnetic Thrust Bearing (MTB), Eddy Current Loss, Fractional Transfer Function, Magnetic Field Intensity, Finite Element Method (FEM)

Introduction

Power losses are inevitable in the operation of active magnetic bearings. They are composed of three parts: hysteresis, eddy current and winding losses. As the most significant component, eddy current loss will be much bigger than two others at high-speed operation. Serious power losses will cause decrease in magnetic force and phase lag between coil current and magnetic force. In order to reduce eddy current loss, laminated structures were used to bearings and rotors. However, it is not suitable for MTBs to use laminated structure and serious eddy current loss will be generated. So it is meaningful to analyze eddy current loss for MTBs.

Several studies have paid more attention to the development of analysis methods for the eddy current loss. Kucera and Ahrens [1] presented an analytical model of eddy currents for a MTB by dividing it into several elementary elements and solving Maxwell equations in each element. The model is very suitable for calculate eddy current loss, magnetic force and other parameters of MTBs. However, the correct boundary conditions were not given and the elementary elements were replaced by semi-infinite plates. So the actual eddy current distributions for MTBs could not be expressed intuitively. Similarly, Sun [2] used the magnetic reluctance to analyze the dynamic stiffness and displacement stiffness of the MTB. By dividing the bearing into six parts according to the flux path, the reluctance of each part could be obtained and the eddy current effects could be considered by the dynamic reluctance. But analytical model of eddy current loss was not constructed. The similar idea were used to these two methods, they divided the MTB into elementary parts. It is convenient to use one-dimensional Maxwell equations to solve eddy current problems. In addition, some other analytical models of eddy current loss for radial magnetic bearings were presented. Allaire [3, 4] proposed a frequency-dependent eddy current loss model, which is related to the number of poles. It is not suitable for analyzing the eddy current loss for MTBs. Sun [5] developed an eddy current loss model for magnetic radial bearings with solid rotor. Ha-Yong [6] presented an analytical model for the eddy-current loss in active magnetic bearing system based on the eddy-current brake concept.

In this paper, based on the ideas of Kucera and Sun [1, 2], the MTB was divided into six parts. A frequency model of eddy current loss for every iron part was presented and the boundary condition was defined by a fractional transfer function with the input of coil current and the output of air-gap magnetic field intensity. FEM harmonic analysis was used to verify the validity of the model.

Modeling

Fig. 1 shows the cross section of a MTB. Except for the coil, the stator, air-gap and disk are divided into 6 element parts according to flux path characters. Part 2 and 5 just have horizontal flux component, however, part 1, 3, 4 and 6 only have vertical flux component. Therefore, one-dimensional Maxwell equations can be easily used to these elementary geometrics.

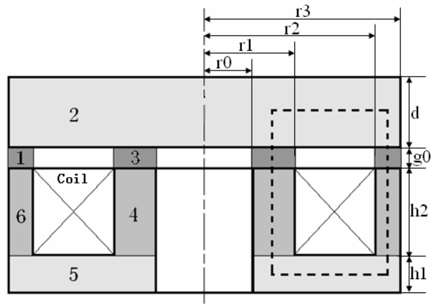

Fig.1. Cross section of a MTB (1 and 3:air gap, 2:thrust disk, 4, 5 and 6:bearing stator)

In order to simplify the analysis, hysteresis, magnetic saturation and leakage are ignored, and only linear and isotropic materials are considered.

Eddy Current Loss for iron parts in a Harmonic Field. One-dimensional eddy current problems can be described using Maxwell's equations [7]. At the same time, displacement current can be neglected because the frequency of coil current of MTBs is sufficiently low. Kucera [1] have developed the distributions of magnetic field intensity for a rotational symmetric plate (such as part 2 or 5) and semi-infinite cylinder (such as part 4 or 6), which can be used to derive the eddy current loss for every iron part.

After solving some Maxwell's equations, the formulas of magnetic field distributions for part 2, 4, 5 and 6 can be written as

$$H_{(2)r}(r,z)=(\frac{e^{\alpha z}}{1+e^{-2\alpha d}}+\frac{e^{-\alpha z}}{1+e^{2\alpha d}})H_{(2)sf} \tag{1}$$

$$H_{(4)z}(r)=\frac{H_{(4)sf}\cdot I_0(\alpha r)}{I_0(\alpha r_1)} \tag{2}$$

$$H_{(5)r}(r,z)=(\frac{e^{\alpha z}}{1+e^{2\alpha h1}}+\frac{e^{-\alpha z}}{1+e^{-2\alpha h1}})H_{(5)sf} \tag{3}$$

$$H_{(6)z}(r) = \frac{K_1(\alpha r_3)I_0(\alpha r) + I_1(\alpha r_3)K_0(\alpha r)}{K_0(\alpha r_2)I_1(\alpha r_3) + I_0(\alpha r_2)K_1(\alpha r_3)} H_{(6)sf} \tag{4}$$

where: $\alpha = \sqrt{j\omega\mu\sigma}$, ω is the angular frequency, μ is the permeability of iron material, σ is the conductivity of iron material, $H_{(k)sf}$ is the surface magnetic field intensity of part k, which will be determined later as boundary condition, $I_j(x)$ is the modified Bessel function of first type and j order and $K_j(x)$ is the modified Bessel function of second type and j order.

According to Ampere's law, the eddy current density for every iron part can be deduced as

$$J_{(2)\varphi}(r,z) = \left(\frac{\alpha}{1+e^{-2\alpha d}} e^{\alpha z} - \frac{\alpha}{1+e^{2\alpha d}} e^{-\alpha z}\right) H_{(2)sf} \tag{5}$$

$$J_{(4)\varphi}(r) = -\frac{\alpha H_{(4)sf}}{I_0(\alpha r_1)} I_1(\alpha r) \tag{6}$$

$$J_{(5)\varphi}(r,z) = \left(\frac{\alpha}{1+e^{2\alpha h1}} e^{\alpha z} - \frac{\alpha}{1+e^{-2\alpha h1}} e^{-\alpha z}\right) H_{(5)sf} \tag{7}$$

$$J_{(6)\varphi}(r) = \frac{\alpha I_1(\alpha r_3)K_1(\alpha r) - \alpha K_1(\alpha r_3)I_1(\alpha r)}{K_0(\alpha r_2)I_1(\alpha r_3) + I_0(\alpha r_2)K_1(\alpha r_3)} H_{(6)sf} \tag{8}$$

When the argument x is large, the simple asymptotic expressions [8] of modified Bessel functions can be obtained

$$I_0(x) \approx I_1(x) \approx \frac{1}{\sqrt{2\pi x}} e^{x} \tag{9}$$

where $-\frac{\pi}{2} < \arg(x) < \frac{\pi}{2}$

$$K_0(x) \approx K_1(x) \approx \sqrt{\frac{x}{2\pi}} e^{-x} \tag{10}$$

where $-\pi < \arg(x) < \pi$

when these approximations are used to the formulas (6) and (8), it will be easily to calculate the eddy current loss for them.

In order to calculate the eddy current loss for every iron part, an infinitesimal volume must be considered. The eddy current loss of an infinitesimal volume can be written as

$$\Delta P = \left|I\right|^2 \cdot \Delta R = \left|(JA)\right|^2 \frac{\Delta l}{\sigma A} = \left|J\right|^2 \frac{1}{\sigma} \Delta V \quad (11)$$

where A is the cross area of eddy current in the infinitesimal volume.

Basing on the formula (11), the volume integral to every iron part in cylindrical coordinate system is carried out. For easy of integration, the cylindrical coordinate system for every part is independent, which have no influence to the calculation results of eddy current loss. After volume integral, the formula of eddy current loss for every iron part are obtained as

$$P_{(2)} = \frac{\pi \left|H_{(2)sf}\right|^2}{\sigma\delta}(1 - e^{-4d/\delta} - 2e^{-2d/\delta}\sin(\frac{2d}{\delta}))(r_2^2 - r_1^2) \quad (12)$$

$$P_{(4)} = \frac{2\pi \left|H_{(4)sf}\right|^2 r_1}{\delta\sigma}(1 - e^{\frac{2(r_0 - r_1)}{\delta}})h_2 \quad (13)$$

$$P_{(5)} = \frac{\pi \left|H_{(5)sf}\right|^2}{\sigma\delta}(1 - e^{-4d/\delta} - 2e^{-2d/\delta}\sin(\frac{2d}{\delta}))(r_2^2 - r_1^2) \quad (14)$$

$$P_{(6)} = \frac{2\pi r_2}{\sigma\delta}\left|H_{(6)sf}\right|^2 (1 - e^{-4(r_3 - r_2)/\delta} - 2e^{-2(r_3 - r_2)/\delta}\sin(2(r_3 - r_2)/\delta))h_2 \quad (15)$$

where $\delta = \sqrt{1/\pi f \sigma\mu}$, which is the skin depth of every iron part.

So the total eddy current loss of the MTB can be written as

$$P_e = P_{(2)} + P_{(4)} + P_{(5)} + P_{(6)} \quad (16)$$

Definition of boundary condition. The magnetic field intensity at the surface of every iron part will be changed because of the influence of eddy current [1]. In this section, the notion of effective reluctance [2] is introduced to determine the boundary conditions.

Previous studies have demonstrated that the magnetic flux will decrease because of the influence of eddy current and which will cause to the reduction of air-gap magnetic field intensity. According to the Ampere circuital theorem, the surface magnetic field intensities of the stator and disk, as the boundary condition of eddy current calculation, will be increased with the reduction of air-gap magnetic field intensity.

Similar to electrical circuit, the definition of magnetic circuit can be used to some problems of electromagnetic field. Reluctance, as a notion of magnetic circuit, can be described as

$$\Re = \Re_r + \Re_i \sqrt{j\omega} \quad (17)$$

where $\Re_r$ is the static reluctance and $\Re_i$ is the coefficient of dynamic reluctance.

After neglecting the effects of hysteresis, magnetic saturation and leakage, the reluctance of every part in Fig.1 can be calculated with formulas in Table 1 and the diagram of magnetic circuit can be shown as Fig. 2 [2].

Table 1
Equivalent reluctance of MTB

	Static reluctance $(\Re_r)$	dynamic reluctance $(\Re_i)$
1	$h_1/(\mu_0 A_{eff})$	0
2	$\ln(r_{2o}/r_{2i})/(2\pi\mu_0\mu_r h_2)$	$\ln(r_{2o}/r_{2i})/(2\pi)\cdot\sqrt{\sigma/(\mu_0\mu_r)}$
3	$h_3/(\mu_0 A_{eff})$	0
4	$h_4/[\pi\mu_0\mu_r(r_{1o}^2 - r_{1i}^2)]$	$h_4/(2\pi r_{4i})\cdot\sqrt{\sigma/(\mu_0\mu_r)}$
5	$\ln(r_{5o}/r_{5i})/(2\pi\mu_0\mu_r h_5)$	$\ln(r_{5o}/r_{5i})/(2\pi)\cdot\sqrt{\sigma/(\mu_0\mu_r)}$
6	$h_6/[\pi\mu_0\mu_r(r_{6o}^2 - r_{6i}^2)]$	$h_6/(2\pi r_{6o})\cdot\sqrt{\sigma/(\mu_0\mu_r)}$

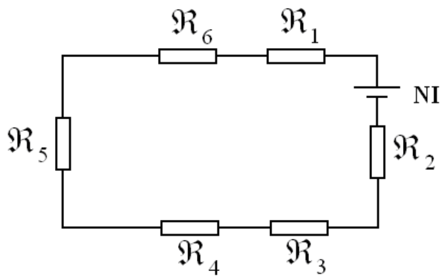

Fig.2. Magnetic circuit of MTB

In order to think about the influence of fringing, the effective area [9] of air gap for the MTB can be described as

$$A_{eff} = \frac{1}{2}(\pi((r_1 + \frac{1}{2}g)^2 - (r_0 - \frac{1}{2}g)^2) + \pi((r_3 + \frac{1}{2}g)^2 - (r_2 - \frac{1}{2}g)^2)) \quad (18)$$

after simplification

$$A_{eff} = A_0(1 + k_g g) \quad (19)$$

where $k_g = \frac{\pi}{2A_0}(r_0 + r_1 + r_2 + r_3)$ and A_0 is the nominal area of air gap.

After the reluctance model is presented, the magnetic flux $\Phi(t)$ in the flux path can be shown as

$$\Phi(t) = \frac{NI(t)}{\Re} \tag{20}$$

where N is the turns of coil, $I(t)$ is the current of the coil and $\Re$ is the reluctance of the flux path.

After uniform flux distribution in the air gap is supposed, the magnetic field intensity of air gap can be written as

$$H_{air}(t) = \frac{NI(t)}{\Re A_{eff}\mu_0} \tag{21}$$

Substituting (17) into (21), the fractional transfer function of the MTB with input $I(t)$ and output $H_{air}(t)$ can be written as

$$\frac{H_{air}(s)}{I(s)} = \frac{N}{A_{eff}\mu_0(\Re_r + \Re_i\sqrt{s})} \tag{22}$$

Transforming equation (22) into time domain, a fractional differential equation can be derived as

$$\frac{d^{(\frac{1}{2})}H_{air}(t)}{dt} + \frac{\Re_r}{\Re_i}H_{air}(t) = \frac{N}{A_{eff}\mu_0\Re_r}i(t) \tag{23}$$

The magnetic field intensity of the air gap can be derived by solving equation (23) with given input current $I(t)$, and the frequency response of (22) also can be easily obtained.

According to Ampere circuital theorem, the surface magnetic field intensity of each iron part with the same material can be calculated by

$$H_{sf}(s) = \frac{NI(s) - H_{air}(s)\cdot 2g_0}{l_{iron}} \tag{24}$$

Simulation

In this part, the eddy current loss of the MTB is researched by FEM analysis. It is assumed that the thrust disk is concentric with the stator and the rotor does not rotate. So a 2-D axisymmetric FEM model is constructed and the FEM software ANSYS 10.0 is used for the analysis.

Fig.3 shows the coupled circuit and magnetic field model of the MTB. An independent current source, a resistor and a stranded coil current source are used in the electric circuit part. Regions A1, A2 and A4 represent the coil, stator and thrust disk, A3, A5, A7 and A9 represent the surrounding air, and A6 and A8 represent the air gap. Fig.4 shows the mesh of the calculation model. There are a total of 4649 elements and 9646 nodes used except for the three elements and four nodes used for the electrical circuit part. In order to improve the accuracy of the calculation at high frequency, very finer mesh is used in the regions near the surface of the stator and disk. The parallel flux boundary condition is applied to the outer boundary of calculation region, therefore, no flux lines will across this boundary.

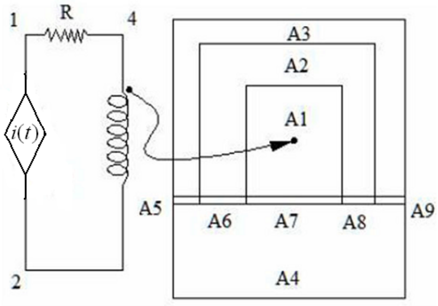

Fig.3. Circuit coupled FEM model

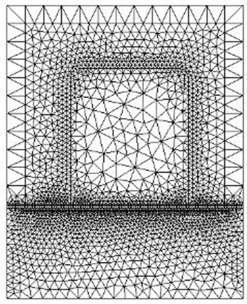

Fig.4. Mesh of the FEM model

In order to verify the validity of the analytical model of eddy current loss for MTB, the harmonic analysis is performed by FEM. Hystersis effect is ignored. The parameters of the calculated MTB are given by Table 2 and Table 3.

Table 2
Dimensions of the MTB

Item	Value	Item	Value
Inner radius of the bearing (r_1)	50mm	Thickness of the back iron (h_1)	5mm
Inner radius of the slot (r_2)	55mm	Length of the slot (h_2)	15mm
Outer radius of the slot (r_3)	68mm	Thickness of the thrust plane (d)	10mm
Inner radius of the bearing (r_4)	72mm	Nominal thickness of the air gap (g_0)	0.5mm

Table 3
Parameters of the test MTB

Item	Value	Item	Value
Relative permeability of iron material (μ_r)	350	Resistivity of iron material (ρ)	$1\times10^{-7}\Omega\cdot m$
Amplitude of coil current (I_0)	1A	Resistivity of the coil (ρ_c)	$2.5462\times10^{-8}\Omega\cdot m$
Resistor of the coil (R)	0.8Ω	Area of the flux path (A_0)	$1704mm^2$
Turns of the coil (N)	86	Length of iron flux path (l_{iron})	56mm

Results

Magnetic field intensity. The frequency responses of the average air-gap magnetic field intensity derived from the results of FEM and frequency model are shown in Fig.5. It shows that the maximum difference between two frequency responses is under15%. So the frequency model for calculating the average air-gap magnetic field intensity is validity.

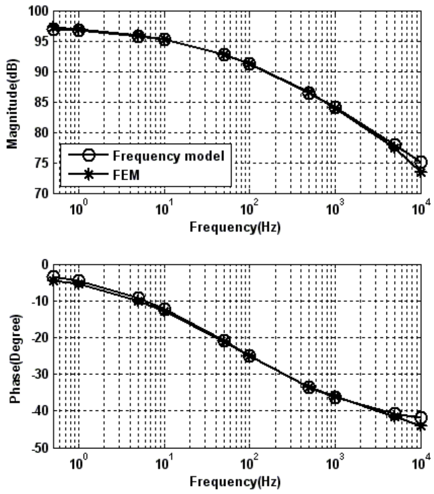

Fig.5 Frequency responses of air-gap magnetic field intensity

Fig.6 shows that the surface magnetic field intensities of the stator and disk increase with the increasing of frequency. The results from two methods are in agreement well with each other when the frequency is limited to 5Hz to 5kHz. Therefore, the method for determining the boundary condition in section 2.2 is reasonable for eddy current loss calculation.

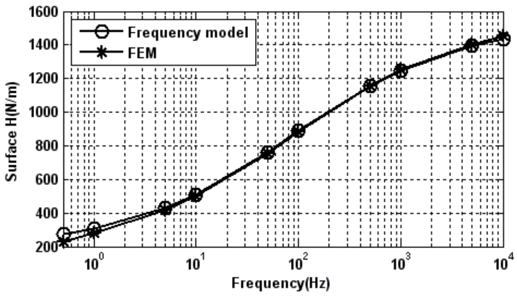

Fig.6 Surface magnetic field intensity of stator and disk

Power losses. The calculation results of eddy current loss from two methods are shown in Fig.7. It can be shown that the eddy current loss will be very serious when the frequency is enough large. And the result from FEM is very close approximation to the result of the frequency model. The difference between them may be caused by the effect of magnetic saturation and leakage. So the frequency model of the eddy current loss for MTB is validity.

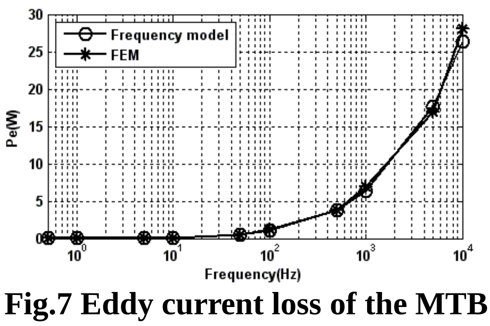

Fig.7 Eddy current loss of the MTB

5 Conclusion

In this paper, a frequency model of eddy current loss was proposed and the average air-gap magnetic field intensity with the different frequency was obtained from a fractional transfer function. The frequency-dependent surface magnetic field intensities of the stator and disk were determined by Ampere circuital theorem as the boundary condition for eddy current loss calculation. Then, the eddy current loss of the MTB was calculated. Finally, FEM results show that the frequency model is reasonable.

Acknowledgements

The work described in this paper was supported by the National Nature Science Foundation, China with Grant No.50635060.

References

[1] L. Kucera and M. Ahrens, A model for axial magnetic bearings including eddy currents, 3rd international symposium on magnetic suspension technology, Tallahassee, 1995.

[2] Y. H. Sun, Y. S. Ho and L. Yu, Dynamic stiff-nesses of active magnetic thrust bearing including eddy current effects, IEEE Trans on Magnetics, 45(2009), 139-149.

[3] M. E. F. Kasarda and P. E. Allaire, Comparison of predicted and measured rotor losses in planar radial magnetic bearings, ASME journal of tribology, 40(1997), 219-226.

[4] P. E. Allaire and M. E. F. Kasarda, Rotor power losses in planar radial magnetic bearings-effects of number of stator poles, air gap thickness and magnetic flux density, ASME journal of engineering for gas turbines and power, 121(1999), 691-696.

[5] Y. H. Sun and L. Yu, Eddy current effects on radial active magnetic bearings with solid rotor, 8th international symposium on magnetic bearings, Japan, 2002.

[6] H. Y. Kim and C. W. Lee, Analysis of eddy current loss for design of small active magnetic bearings with solid core and rotor, IEEE Trans on Magnetics, 40(2004), 3293-3301.

[7] R. L. Stoll, The analysis of eddy currents, London, Oxford university press, 1974.

[8] W. Magnus, F. Oberhettinger and R. P. Soni, Formulas and theorems for the special function of mathematical physics, New York: Springer-verlag, 1962.

A. R. Hambley, Electrical engineering: principles and applications, Pearson education, 2007.